Cancer Letters 453 (2019) 158–169

Contents lists available at ScienceDirect

Cancer Letters

journal homepage: www.elsevier.com/locate/canlet

Original Articles

CD90 highly expressed population harbors a stemness signature and creates an immunosuppressive niche in pancreatic cancer

Juanjuan Shi[a], Ping Lu[a], Wenyan Shen[b], Ruizhe He[c], Min-Wei Yang[c], Yuan Fang[d], Yong-Wei Sun[c,***], Ningning Niu[a,**], Jing Xue[a,*]

[a] State Key Laboratory of Oncogenes and Related Genes, Stem Cell Research Center, Renji Hospital, Shanghai Cancer Institute, School of Medicine, Shanghai Jiao Tong University, Shanghai, China
[b] Department of Clinical Laboratory, Renji Hospital, School of Medicine, Shanghai Jiao Tong University, Shanghai, China
[c] Department of Biliary-Pancreatic Surgery, Renji Hospital, School of Medicine, Shanghai Jiao Tong University, Shanghai, China
[d] Department of General Surgery & Research Institute of Pancreatic Disease, Ruijin Hospital, School of Medicine, Shanghai Jiao Tong University, Shanghai, China

ARTICLE INFO

Keywords:
Pancreatic ductal adenocarcinoma (PDAC)
CD90/Thy1
Stemness
Monocyte/macrophage
Immunosuppressive

ABSTRACT

Pancreatic ductal adenocarcinoma (PDAC) is a highly aggressive disease with no effective treatment. Cancer cells, especially cancer stem cells (CSCs), redirect immune cells to evade immune surveillance and even coopt these immune cells to support their growth and metastasis. However, the identification of CSCs and how CSCs interact with immune cells in PDAC remain uncharacterized. Here, we report that CD90 is expressed on both stromal and tumor cells and that high expression of CD90 is related to a poor prognosis in patients with PDAC. The CD90 highly expressed ($CD90^{hi}$) population in PDAC cells harbors high stemness features and tumorigenicity. Notably, CD90 acts as an anchor for monocyte/macrophage adhesion, providing a physical interaction between $CD90^{hi}$ cells and monocytes/macrophages. In response, the crosstalk between $CD90^{hi}$ cells and monocytes/macrophages promotes immunosuppressive features of immune cells, which enhance the stemness and epithelial-mesenchymal transition (EMT) of PDAC cells. Moreover, PD-L1 is dominantly expressed in the $CD90^{hi}$ population, providing another strategy for these cells to evade immune surveillance. These findings provide an understanding of the biological significance of CD90 expression in PDAC cells and uncover a novel mechanism for how "stem-like" PDAC cells evade immune surveillance.

1. Introduction

Pancreatic ductal adenocarcinoma (PDAC), the most common form of pancreatic tumors, is characterized by a highly malignant and poor prognosis, with a five-year survival rate of less than 8% [1–3]. Despite recent advances in diagnosis and surgery, the survival of PDAC patients has changed little in the past two decades. Cancer stem cells (CSCs), defined by their abilities to self-renew, repopulate and undergo *in vivo* tumorigenicity, are believed to contribute to tumor initiation, relapse and therapeutic resistance [4–6]. Therefore, the identification and mechanistic study of CSCs are urgently needed.

An immunosuppressive microenvironment is a common feature in PDAC. Tumor cells, especially CSCs, redirect immune cells to evade immune surveillance and even coopt immune cells to support their growth and metastasis [7,8]. Monocytes and derived macrophages, which are abundant in both clinical and experimental PDAC tissue, have been proved to be indispensable for the initiation and metastasis of pancreatic cancer [9–13]. However, the crosstalk between pancreatic CSCs and adjacent immune cells is still elusive. Investigation of the crosstalk between CSCs and immune cells would reveal how CSCs respond to cues from their surroundings for disease progression.

CD90, also named Thy-1, is a 25–37 kDa glycosylphosphatidylinositol (GPI)-anchored glycoprotein expressed in various cell types, including hematopoietic stem cells, activated microvasculature endothelial cells and fibroblasts, and is mainly responsible for cell adhesion, migration and fibrosis [14,15]. Moreover, CD90 has been reported to be expressed on tumor-initiating cells in several solid tumors [16–20]. However, except for reports about CD90 expression in PDAC

* Corresponding author. State Key Laboratory of Oncogenes and Related Genes, Stem Cell Research Center, Renji Hospital, School of Medicine, Shanghai Jiao Tong University, 160 Pujian Rd, Shanghai, 200127, China.
** Corresponding author. Stem Cell Research Center, Renji Hospital, School of Medicine, Shanghai Jiao Tong University, 160 Pujian Rd, Shanghai, 200127, China.
*** Corresponding author. Department of Biliary-Pancreatic Surgery, Renji Hospital, School of Medicine, Shanghai Jiao Tong University, 160 Pujian Rd, Shanghai, 200127, China.
E-mail addresses: syw0616@126.com (Y.-W. Sun), niunn2014@outlook.com (N. Niu), jingxue@sjtu.edu.cn (J. Xue).

https://doi.org/10.1016/j.canlet.2019.03.051
Received 12 October 2018; Received in revised form 28 March 2019; Accepted 28 March 2019

stroma [21,22], little is known about the expression pattern of CD90 in pancreatic cancer cells and its potential role in PDAC tumorigenesis.

These considerations prompted us to identify “stem-like” cells in PDAC and to explore the mechanism by which tumors survive and evade immune surveillance. Here, we show that CD90 is expressed on both stromal and tumor cells in PDAC tissues, and its high expression is linked to a poor prognosis. PDAC cells with high expression of CD90 harbor stemness characteristics. Notably, CD90 acts as an anchor for monocyte/macrophage adhesion in PDAC cells, providing crosstalk between $CD90^{hi}$ PDAC cells and monocytes/macrophages in a near-secretory manner. Moreover, $CD90^{hi}$ PDAC cells express high levels of PD-L1 and suppress the T cell response. Thus, $CD90^{hi}$ PDAC cells harbor stemness properties and create an immunosuppressive niche, which enhances the stemness and epithelial-mesenchymal transition (EMT) state of PDAC. These results provide invaluable insights and new therapeutic strategies for the diagnosis and treatment of PDAC.

2. Materials and methods

2.1. Cell culture

Human pancreatic cancer cell lines (SW1990, PANC1, MiaPaCa2, AsPC-1 and HPAC) were purchased from the American Type Culture Collection (ATCC). SW1990, PANC1 and MiaPaCa2 cells were cultured in high glucose Dulbecco's Modified Eagle Medium (DMEM), and AsPC-1 and HPAC cells were cultured in RPMI 1640 medium and a 1:1 mixture of DMEM and F12, respectively, containing 10% fetal bovine serum (FBS) and 1% penicillin-streptomycin. Pancreatic patient-derived tumor cells (PDCs), including PDC0034 and PDC0049, were isolated from pancreatic PDX (patient-derived xenograft) tumors and cultured in complete RPMI 1640 medium plus 10 ng/ml EGF (Epidermal growth factor) and 1% insulin-transferrin-selenium (ITS) as previously described [23]. Human pancreatic tissue specimens were derived from patients with confirmed diagnoses of pancreatic ductal adenocarcinoma (PDAC) at Renji Hospital. Primary tumor cells from PDAC patient samples were directly isolated by collagenase digestion (collagenase IV, 2 mg/ml, 30–60 min). THP-1 cells were obtained from the ATCC and grown in RPMI 1640 medium supplemented with 10% FBS, 1% penicillin-streptomycin and 5 mM β-mercaptoethanol. All cells were cultured in a humidified incubator at 37 °C with 5% CO2.

For the coculture experiment, tumor cells and THP-1 cells (2:3) were cultured together for 36 h in DMEM supplemented with 10% FBS. Primed PDAC cells or THP-1 cells were sorted for further use. Control cells underwent the same sorting process.

2.2. Flow cytometry

Cells were prepared as a single-cell suspension for FACS staining. For CD90 staining, cells were stained with APC-CD90 antibody (Clone #5E10, Biolegend) for 30 min at 4 °C. $CD90^{+}$ and $CD90^{-}$ cells were identified based on isotype gating. ALDH activity was determined by the ALDEFLUOR Kit following the manufacturer's instructions (STEM CELL). The stained cells were acquired for analysis or sorted on an LSRFortessa or a FACS Aria II flow cytometer (BD). Flow cytometry data were analyzed with FlowJo software (Tree Star Inc.).

2.3. Quantitative RT-PCR

Total RNA was extracted from the indicated cells using Trizol (Invitrogen) according to the manufacturer's protocol. cDNA was synthesized using the High Capacity cDNA Reverse Transcription Kit (Applied Biosystems). Specific primers are included in the supplementary information (Supplement Table 1). Quantitative RT-PCR was performed with SYBR Green Master Mix (Roche) on a Step One Plus system (Applied Biosystems). The relative expression of target genes was calculated according to the Ct value with normalization to GADPH.

2.4. Sphere formation assay

Sphere culture was performed as previously described [24,25]. Briefly, cells were plated in 24-well Ultra-Low Attachment Plates (Corning) with DMEM: F12 medium plus 2% B27 (Gibco) and 20 ng/ml bFGF (PeproTech). The culture medium was replenished every 3 days. After 7 days, the sphere diameter and number (> 50 μm) were evaluated and quantified.

2.5. Monocyte adhesion assay

For the monocyte adhesion experiment, pancreatic cancer cells were seeded at 70–80% confluency before adding THP-1 monocytes (THP-1:PDAC cells = 3:2). The non-adherent monocytes were gently rinsed away with PBS after 1 h of coculture, and then the remaining cells in the culture dish were trypsinized and stained with the indicated antibody for flow cytometry.

2.6. PBMC isolation and in vitro culture

PBMCs (peripheral blood mononuclear cells) were isolated by density gradient centrifugation from healthy donors using Ficoll-Hypaque. Prepared PBMCs were seeded in 96-well round bottom plates and then treated with PDAC conditioned medium for 6 days before staining and flow cytometry analysis. DAPI (Life Technology) was used to exclude dead cells.

2.7. Immunohistochemistry (IHC) and immunofluorescence (IF)

Pancreas tissues were fixed in 10% buffered formalin or frozen in Tissue-Tek OCT compound. Fixed and frozen tissues were sectioned for IHC and IF, respectively, using CD90 (Abcam, 133350), CD68 (Abcam, ab955), CD68 (Biolegend, #Y1/82A) and CD8 (Abcam, ab93278). Cells were mounted with DAPI and prolonged gold antifade reagent (Thermo Fisher Scientific) before analysis with a confocal microscope.

2.8. Lentiviral transduction

The CD90 gRNA expression oligos and control oligos were introduced into LentiCRISPR V2 (Addgene). The sequences of these oligos are shown in Supplementary Table 1. A lentivirus containing the CD90 gRNA sequence and the control gRNA sequence was transfected into PANC1 cells. After 2 weeks of selection with puromycin (2 μg/ml), multiple colonies were picked and passaged for sequencing. Knockout efficiency was determined by qPCR and flow cytometry.

2.9. Cell viability analysis

Cell proliferation and gemcitabine sensitivity assays were performed with CellTiter-Glo® 2.0 reagent (Promega) according to the manufacturer's instructions.

2.10. Migration and invasion assays

Transwell-based cell migration and invasion assays were performed in polyethylene terephthalate-based migration chambers with an 8 μm pore size according to the manufacturer's instructions. The 1:8 mixture of Matrigel and serum-free DMEM was plated onto filters in the upper chambers one hour in advance when the invasion assay was performed. Then, tumor cells (5×10^3) in serum-free DMEM were seeded onto filters in the upper chambers, while DMEM containing 10% FBS was added to the lower chambers. After 36 h of incubation for the migration assay and 48 h of incubation for the invasion assay, cells on the upper surface of the filters were removed, and filters were fixed with 4% PFA and stained with crystal violet. After imaging, the stained cells were stained with acetic acid to detect the absorbance at OD595.

2.11. In vivo tumor formation

The indicated numbers (10^3 each) of $CD90^-$ and $CD90^{hi}$ cells sorted from PANC1 cells were subcutaneously transplanted into nude mice (from Shanghai SLAC Laboratory Animal Co., Ltd.). Tumor incidence was monitored for 8 weeks. All animals were maintained and used in accordance with the guidelines of the Institutional Animal Care and Use Committee of the Renji Hospital.

2.12. T cell proliferation assay

$CD4^+$ and $CD8^+$ T cells were isolated and sorted from the fresh human peripheral blood of healthy volunteers. Then, enriched $CD4^+$ and $CD8^+$ T cells were labeled with 1.0 μM CFSE (Invitrogen) in PBS and incubated at 37 °C for 30 min as previously described [26]. The cells were cultured at $5*10^4$ cells per well in 96-well round bottom plates and then activated with anti-CD3 and anti-CD28 antibodies (2 μg/ml each) for 5 days under different conditions.

2.13. Statistics

The Pearson correlation together with the P value was computed to measure the correlation between the indicated genes. The survival curve was estimated by the Kaplan-Meier method. Two-way ANOVA or one-way ANOVA together with Bonferroni's post hoc test was used for multiple group analysis. An unpaired Student's t-test was used to determine statistical significance in the rest of the experiments, and a P value of less than 0.05 was considered significant. Values are expressed as the mean ± SEM or the mean ± SD (Prism 6; GraphPad Software). Unless indicated, the results were obtained from at least two or three independent experiments.

3. Results

3.1. CD90 is upregulated in pancreatic cancer and expressed on both stromal and tumor cells

To determine the expression level of CD90 in PDAC (pancreatic ductal adenocarcinoma), we analyzed gene expression from 4 published databases, TCGA (PAAD), GSE15471 [27], GSE28375 [28] and GSE102238 (Renji cohort) [29]. Notably, the expression of CD90 was significantly higher in PDAC than in adjacent normal tissues (Fig. 1A). Previous studies have shown that CD90 is expressed on PDAC stroma cells, such as fibroblasts and vascular endothelial cells [21,22]. To further elucidate the distribution of CD90 in PDAC, we performed immunohistochemical staining for CD90 using a tissue array. In line with previous reports, we observed that CD90 was dominantly expressed on PDAC stromal cells (34.74%), whereas CD90 could also be detected on tumor cells in a small portion of PDAC patients (10%) (Fig. 1B). Moreover, the expression of CD90 gradually increased from normal tissues to intraepithelial neoplasia (PanINs) and PDAC in the GSE43288 familial pancreatic cancer database [30] (Fig. 1C).

To further verify the expression of CD90 on PDAC cells, we examined its surface level with flow cytometry on cell lines, PDCs (PDX-derived cancer cells, generated from patient-derived xenografts) and primary cells (freshly isolated from patients' tumors). Flow cytometry analysis revealed that CD90 expression was limited to a small subset of PDAC cells, which are referred to as $CD90^{hi}$ PDAC cells (Fig. 1D, Figure S1 A-B). The above data confirmed the expression of CD90 in pancreatic tumor cells.

Next, we sought to explore which signaling pathway CD90 might be involved in, and we performed GSEA using TCGA (PAAD) database. We grouped patients according to the median mRNA expression of CD90, in which the top 80% was defined as $CD90^{hi}$ and the bottom 20% was defined as $CD90^{low}$. The results revealed that the pathways associated with PDAC malignance/aggressiveness were positively enriched in $CD90^{hi}$ cells (versus control $CD90^{low}$ cells), including Kras signaling, epithelial mesenchymal transition (EMT), IL-6/JAK/STAT3 signaling and TNFα signaling via NFκB (Fig. 1E). Moreover, the high expression of CD90 was significantly associated with poor survival in TCGA (PAAD) database (Fig. 1F). The above data suggest that increased CD90 expression may be an important predictor of poor survival in pancreatic cancer.

To further elucidate which signaling pathway might participate in the regulation of CD90 levels, we treated PANC1 cells with inhibitors specific to Wnt, Notch, Hedgehog (Gli), Hippo (YAP1), STAT3 and mTOR signaling. Here, we found that only Gli1 and YAP1 inhibitors could partially reduce CD90 expression at both the protein and mRNA levels (Figs. S1C–D). Furthermore, CD90 expression was positively correlated with the expression of Gli1 and YAP1 in TCGA (PAAD) database (Fig. S1E), suggesting that the Sonic Hedgehog and Hippo-YAP pathways might participate in the regulation of CD90 expression in PDAC.

3.2. $CD90^{hi}$ PDAC cells harbor stemness properties

Previous studies have shown that CD90 is a surface marker that can be used to define cancer stem cells in various tumors [16–20]. However, the role of CD90 in PDAC is still not well defined. To annotate the function of CD90 in PDAC, we first performed gene set enrichment analysis (GSEA) with the PDAC database by dividing PDAC patients into 2 groups according to the median expression of CD90 ($CD90^{hi}$ vs $CD90^{low}$). Compared with $CD90^{low}$, $CD90^{hi}$ PDAC showed a significant enrichment of genes related to mammary stem cells (Fig. 2A). Moreover, to determine whether high expression of CD90 was associated with stemness in PDAC, pancreatic cancer stem cells (CSCs) were enriched in nonadherent, serum-free, growth factor-supplemented conditions *in vitro* as previously reported [24,25]. We observed that CD90, along with other multiple stemness-related genes (*NANOG, SOX2* and *POU5F1*), especially *SOX2*, was significantly higher in spheres compared to adherent monolayer cells (Fig. 2B, Fig. S2A), suggesting that CD90 is associated with cancer stemness in PDAC. In addition, the expression of CD90 was positively correlated with SOX2 expression in the Renji PDAC cohort (Fig. S2B).

Aldehyde dehydrogenase A1 (ALDHA1) is an operative and well-recognized stemness marker. We found that $CD90^{hi}$ cells exhibited higher ALDH activity than $CD90^-$ cells in multiple PDAC cell lines (Fig. 2C and Fig. S2C). To further discern these two populations in PDAC, we used flow cytometry to purify PDAC cells based on CD90 expression. Quantitative RT-PCR analysis revealed that the expression levels of core stemness genes (NANOG, SOX2 and POU5F1) were higher in $CD90^{hi}$ cells than in $CD90^-$ cells (Fig. 2D, Fig. S2D). Moreover, $CD90^{hi}$ cells had higher clonogenic capability than the $CD90^-$ population according to the sphere assay (Fig. 2E, Fig. S2E). However, the growth rate of $CD90^{hi}$ cells was comparable to that of $CD90^-$ cells, indicating that the observed differences were not related to the changes in proliferation rate (Fig. 2E). In addition, $CD90^{hi}$ cells possessed stronger resistance to gemcitabine *in vitro* (Fig. S2F). To determine the *in vivo* tumorigenic potential of the two subpopulations, 10^3 $CD90^{hi}$ and $CD90^-$ cells sorted from PANC1 cells were subcutaneously transplanted into immunodeficient mice. Eight weeks after injection, we found that $CD90^{hi}$ cells possessed higher tumorigenicity (Fig. 2F). Thus, the $CD90^{hi}$ population widely existed in PDAC cells and displayed stemness properties.

3.3. CD90 acts as an anchor for monocyte/macrophage cell adhesion in PDAC cells

CD90 is a GPI-anchored glycoprotein that has been shown to interact with integrins displayed by adjacent cells, such as the monocyte/macrophage surface marker CD11b/MAC-1 (integrin alpha M/beta) [31]. CD90, expressed on breast cancer stem cells, was shown to

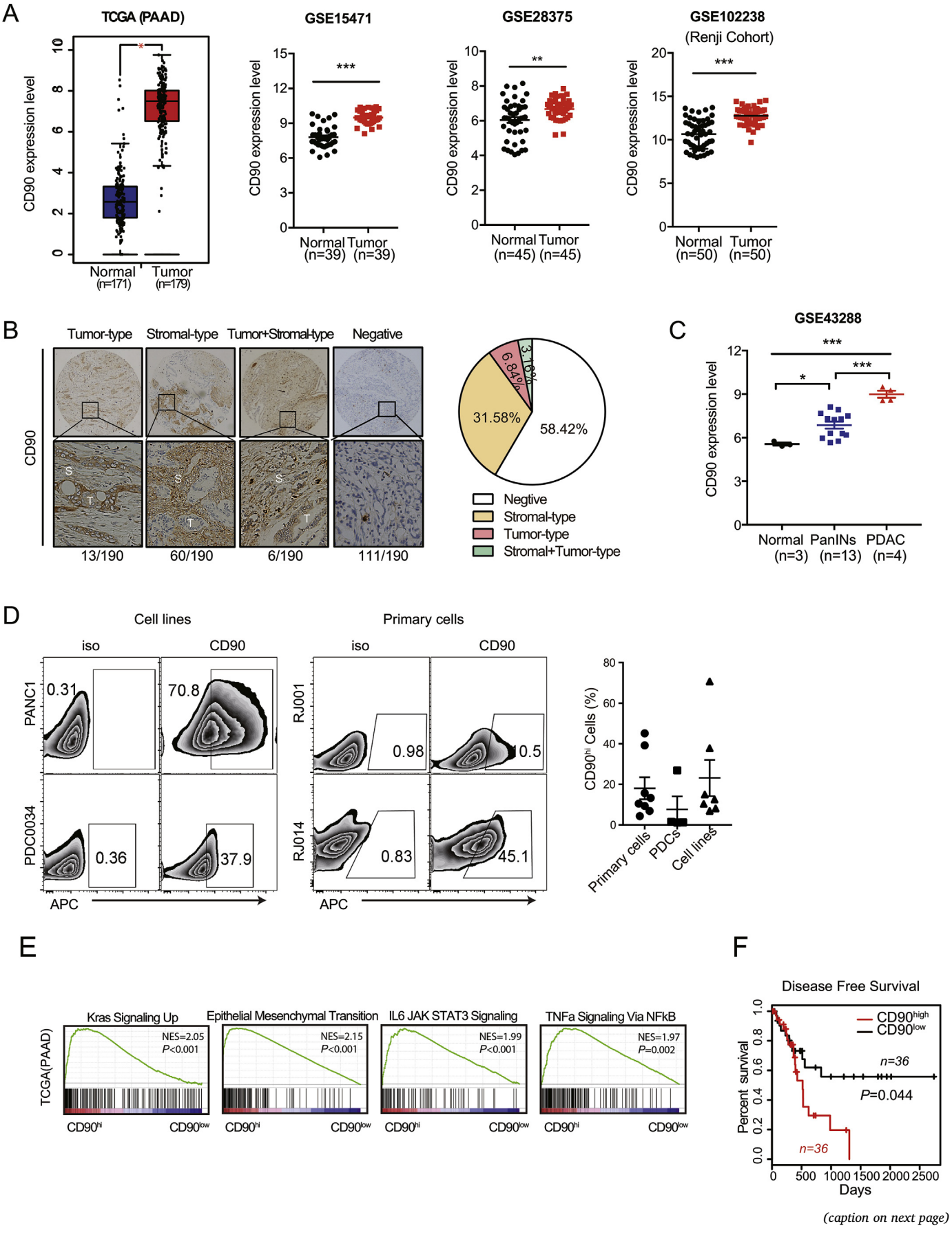

(caption on next page)

Fig. 1. CD90 is upregulated in pancreatic cancer. (A) Relative mRNA level of CD90 in the pancreas is shown. Data were collected from TCGA (PAAD), GSE15471, GSE28375 and GSE102238 (Renji cohort) (mean ± SEM, unpaired two-tailed Student's t-test). (B) Representative immunohistochemical images of CD90 in a PDAC tissue array. S, stromal cell; T, tumor cell. (C) The expression of CD90 was detected in normal (n = 3), PanINs (n = 13) and PDAC (n = 4) tissues isolated from familial pancreatic cancer in the public GSE43288 database (mean ± SEM, unpaired two-tailed Student's t-test). (D) Flow cytometry analysis of CD90 expression among PDAC cell lines, PDCs and primary tumor cells (pregated on live$^+$ EpCAM$^+$ cells). (E) GSEA revealed that CD90^{hi} cells (versus control CD90^{low} cells) were positively enriched for Kras signaling, epithelial mesenchymal transition, IL6/JAK/STAT3 signaling and TNFα signaling via NFκB. Data were collected from TCGA (PAAD) database. (F) The association between CD90 transcript level and overall survival in PDAC patients is shown. The analyses were conducted in 179 pancreatic cancer patients from TCGA database (log-rank test $P = 0.044$).

mediate the physical interaction between CSCs and macrophages, which could facilitate CSCs to maintain their stem-like state [16]. We speculated that CD90 might serve as an anchor for CD90^{hi} PDAC cells to tether monocytes and derived macrophages in PDAC. First, GSEA from TCGA (PAAD) database revealed that the integrin-associated pathway was enriched in CD90^{hi} cells (Fig. 3A). Next, we analyzed the correlations between CD90 and monocyte/macrophage-associated genes, including CD14, CD68, MRC1 and CD163. Notably, CD90 expression was positively correlated with the expression of CD14, CD68, MRC1 and CD163 in both TCGA database (Fig. 3B) and the Renji cohort (Fig. S3A). The above results suggest that CD90 expression is associated with the existence of monocytes/macrophages.

In support of this notion, we employed the human monocytic cell line, THP-1. Multiple PDAC cell lines were expanded early in monolayer culture, and then suspended THP-1 cells were added above the cell monolayers for the adhesion assay. CD45, a well-known marker of immune cells, was used to distinguish tumor cells from THP-1 cells (Fig. 3C). Notably, we found that the adhesion capability of PDAC cell lines to THP-1 monocytes was related to their surface CD90 level (Fig. 3D). Moreover, we found that macrophages (CD68) are in close proximity to CD90^{hi} cells in clinical pancreatic tumor tissues by immunofluorescence staining (Fig. S3B). To further validate the role of CD90 in the adhesion of monocytes/macrophages, we next generated CD90-knockout PANC1 cells using the CRISPR-Cas9 system (Fig. 3E). Knockout of CD90 dramatically reduced the adhesion to THP-1 monocytes in PANC1 cells (Fig. 3F) but had little effect on cell proliferation (Fig. S3C). The above results suggest that CD90 could act as an anchor for monocyte/macrophage adhesion in PDAC cells.

3.4. PDAC cells promote immunosuppressive features of monocytes/macrophages

To explore the crosstalk between PDAC cells and attached monocytes/macrophages, we generated a coculture system with PDAC and THP-1 cells (Fig. 4A). After coculture for 36 h, we sorted the primed THP-1 cells for quantitative RT-PCR analysis. Surprisingly, we found that the expression of SHH, IL-6, IL8 and IL-10 in THP-1 cells was upregulated following coculture with PDAC cells (Fig. 4B). Among them, IL-6 and IL-10 are related to the immunosuppressive properties of monocytes/macrophages. Furthermore, PBMCs (peripheral blood mononuclear cells) were treated with conditioned medium from human PDAC cells and then harvested 5 days later for flow cytometry analyses. The ratio of CD14$^+$ monocytes was strongly elevated under PDAC conditioned medium treatment (Fig. 4C). Moreover, primed CD14$^+$ monocytes acquired an immunosuppressive feature characterized by significantly reduced expression of HLA-DR (Fig. 4D) and higher expression of IL-6 and IL-10 (Fig. 4E). To further determine the immunosuppressive feature of PDAC-primed monocytes, we cultured CD4$^+$ and CD8$^+$ T cells with naïve THP-1 or PDAC-primed THP-1 cells. In this functional assay, we found that the proliferation of T cells (both CD4$^+$ or CD8$^+$ T cells) was significantly impaired when cocultured with PDAC-primed THP-1 cells compared to naïve THP-1 cells (Fig. 4F). Furthermore, by immunostaining of CD90 together with monocyte/macrophage and T cell markers, we found that high expression of CD90 on PDAC cells was accompanied by abundant macrophages (CD68$^+$) and few CD8$^+$ T cells (Fig. 4G). Thus, PDAC cells trapped monocytes/macrophages by the CD90/CD11b (MAC-1) axis and reprogrammed them into immunosuppressive states.

3.5. Monocytes/macrophages promote stemness and the EMT of PDAC cells

As cancer progresses, tumor cells may reprogram the surrounding cells to create a supportive microenvironment that facilitates their growth and metastasis. Monocyte and derived macrophages determine the initiation and metastatic processes of PDAC [8–13]. However, little is known about the crosstalk between monocytes/macrophages and pancreatic CSCs. Here, we wondered whether tethered monocytes/macrophages by CD90^{hi} PDAC cells could contribute to their stemness maintenance and metastasis. Based on the above coculture system, PDAC cells cocultured with or without THP-1 cells were sorted for multiple assays. Here, we found that the expression of core stemness genes (*SOX2*, *NANOG*, *POU5F1*) and EMT-related genes (*ZEB2*, *TWIST1*) in PDAC cells was highly upregulated after coculture with THP-1 cells compared with those cultured alone (Fig. 5A). Moreover, increased expression of SOX2 and ZEB2, as well as reduced E-cadherin was further confirmed at the protein level (Fig. 5B).

In addition, the sphere assay further confirmed that coculture with THP-1 cells enhanced the stemness of PDAC cells (Fig. 5C). We reasoned that direct contact of monocytes/macrophages with CD90^{hi} cells might allow monocytes/macrophages to provide near-signals, which are crucial for PDAC cells to maintain their stemness. To test this hypothesis, PDAC cells were treated with conditioned medium from THP-1 monocytes. Here, we found that stemness-related genes, especially SOX2, were upregulated in PDAC cells (Fig. S4A). In addition, conditioned medium from THP-1 cells had a comparable ability to promote the stemness of PDAC cells according to sphere formation and ALDH activity (Fig. 5D and E). By analyzing medium from THP-1 cells, we noticed that IL8 was the most abundant cytokine (Fig. S4B). Moreover, PDAC cells could promote monocytes to express even more IL8, as shown in Fig. 4. Consistent with previous reports [32–34], we found that IL8 could enhance the stemness of PDAC cells, as confirmed by stemness-related gene expression, sphere formation and ALDH activity (Figs. S4C–E). To further determine whether THP-1 cell-promoted PDAC stemness was mediated by IL8, we blocked IL8 with its neutralizing antibody. Notably, ALDH activity enhanced by THP-1 CM in PDAC cells was largely abrogated after neutralization with the IL8 antibody (Fig. 5F).

As shown in Fig. 5A, the crosstalk between THP-1 monocytes and PDAC cells also enhanced the expression of EMT-related genes. Consistent with the qPCR assay, PDAC cells cocultured with THP-1 cells gained higher migrative and invasive capabilities (Fig. 5G). SHH, a ligand of sonic hedgehog signaling, was dramatically induced in PDAC-primed THP-1 monocytes (THP-1 monocytes cocultured with PDAC) (Fig. 4). Consistent with previous reports [35,36], we found that SHH could promote PDAC migration (Fig. 5H). To further explore the involvement of SHH/Gli signaling in the crosstalk between PDAC cells and THP-1 monocytes, SW1990 cells cocultured with THP-1 monocytes were treated with DMSO or GANT61 (a specific inhibitor of Gli1/2). After coculture for 36 h, SW1990 cells from the DMSO/GANT61-treated groups were sorted for the Transwell migration assay. Notably, blocking SHH/Gli signaling with GANT61 could impair the migration of SW1990 cells, suggesting that SHH is involved in the crosstalk between

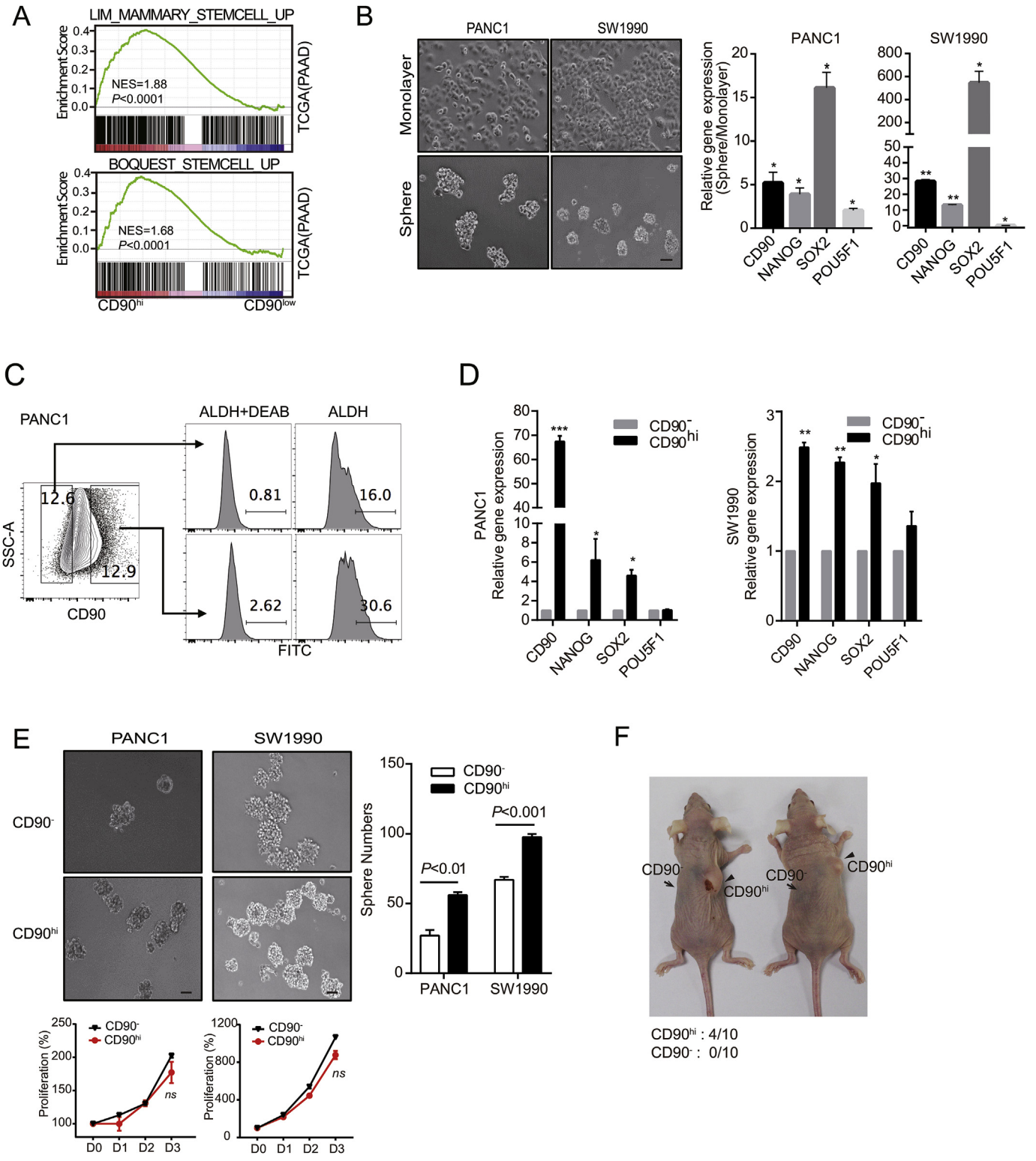

Fig. 2. CD90^{hi} PDAC cells harbor stemness properties. (A) GSEA showed that CD90^{hi} cells were positively enriched for stem cells versus CD90^{low} cells in TCGA (PAAD) database. (B) PANC1 and SW1990 cells were grown as monolayers and spheres. qPCR analysis of stemness-associated genes and CD90 expression in spheres versus adherent cells. Data were normalized to GAPDH expression and are presented as the fold change relative to adherent cells. (C) ALDEFLUOR analyses of CD90^{hi} and CD90^{-} cells from PANC1 cells. DEAB, a specific inhibitor of ALDH1, was used as a control. (D) CD90^{hi} and CD90^{-} cells were sorted with flow cytometry. The relative expression of CD90 and stemness-associated genes was determined by qPCR. Data are shown as the mean ± SEM, n = 3, *P < 0.05 (multiple unpaired Student's t-test). (E) CD90^{hi} and CD90^{-} cell subpopulations from PANC1 and SW1990 cells were sorted for sphere assay and colony formation. The mean number of spheres and proliferation between two groups are shown. Scale bar: 50 μm. (F) CD90^{hi} and CD90^{-} cells (10^3 each) sorted from PANC1 cells were injected subcutaneously into two sides of BALB/c nude mice. After 2 months, CD90^{hi} cells, but not CD90^{-} cells, formed tumor nodules. Arrows indicate the sites of injection (n = 10 per group). All data are shown as the mean ± SEM from three independent experiments, *P < 0.05, **P < 0.01, ***P < 0.001 (unpaired two-tailed Student's t-test).

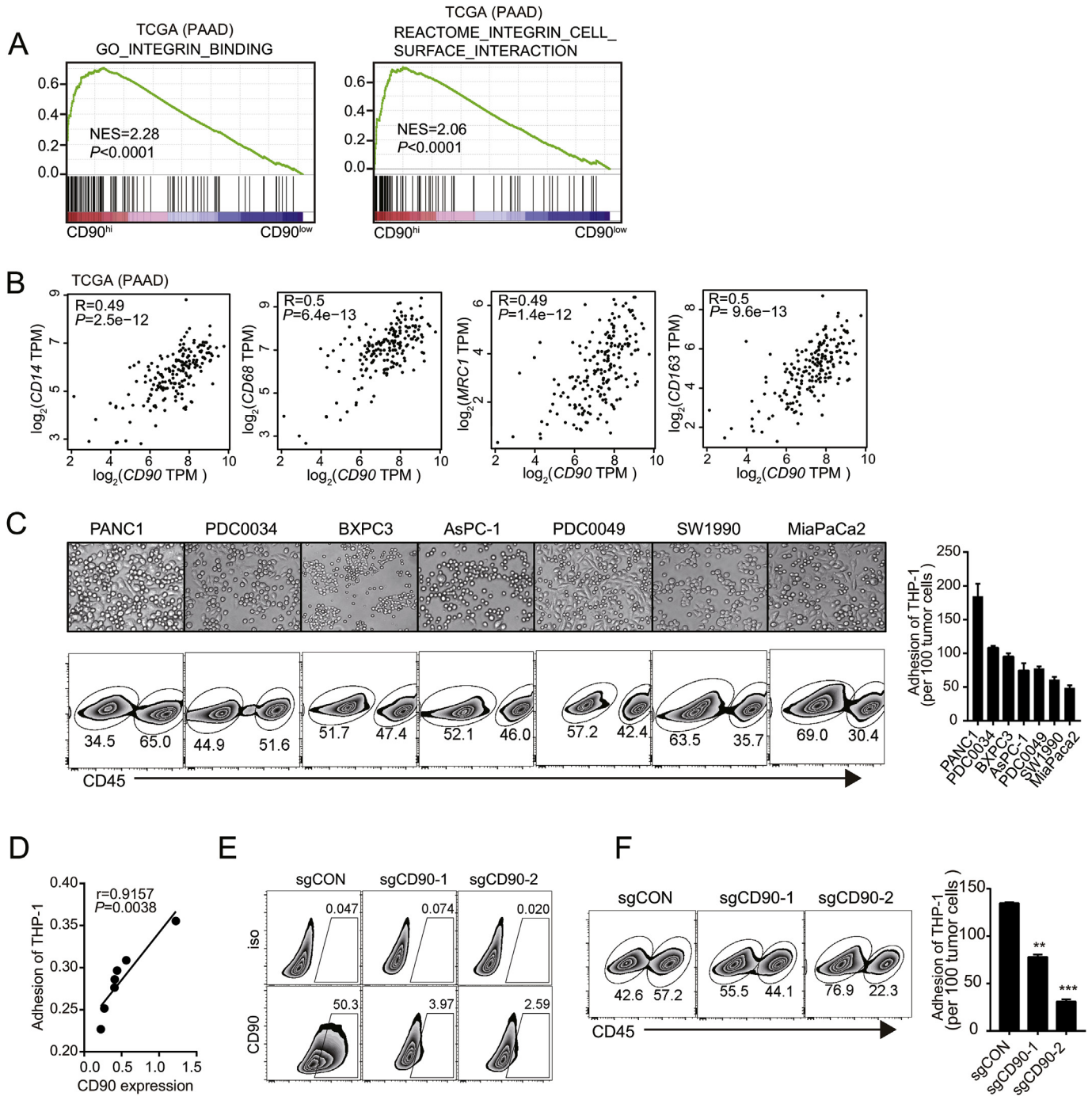

Fig. 3. CD90 acts as an anchor for monocyte/macrophage adhesion in PDAC cells (A) GSEA revealed that CD90^{hi} cells (versus control CD90^{low} cells) were positively enriched for integrin binding and integrin cell surface interaction. Data were collected from TCGA (PAAD) database. (B) Plots show significant correlations between monocyte/macrophage-associated genes (CD14, CD68, MRC1 and CD163) and CD90 expression in TCGA (PAAD) database. (C) THP-1 monocytes were cultured with PDAC cells. Monocytes that did not adhere to the PDAC monolayer were washed away after 1 h. Attached monocytes were quantified by flow cytometry based on CD45 expression. Representative images and flow cytometry profiles are shown on the left. The ratios of attached monocytes are shown on the right. (D) CD90 expression ($\log_{10}$ transformed MFI) was positively associated with the adhesion of THP-1 monocytes. (E) CD90 knockout efficiency in PANC1 cells was examined by flow cytometry. (F) Representative flow cytometry profiles of THP-1 cells adhered to PANC1 sgCD90 and sgCON cells are shown on the left. The ratios of attached THP-1 cells were calculated and are shown on the right. Data are shown as the mean ± SEM, $^{**}P < 0.01$, $^{***}P < 0.001$.

PDAC cells and THP-1 monocytes (Fig. 5H).

3.6. CD90^{hi} PDAC cells exhibit high PD-L1 expression and suppress T cell proliferation

As shown above, CD90^{hi} PDAC cells with high stemness properties tethered and reprogrammed monocytes/macrophages into an immunosuppressive state. In turn, these monocytes/macrophages further promoted the stemness and EMT of PDAC cells. Creating an immunosuppressive niche is a strategy for tumor cells, especially CSCs, to evade immune surveillance [13,37]. It is well known that the PD-L1/PD-1 axis drives T cell dysfunction and exhaustion, thus enabling tumor cells to escape immune surveillance. Surprisingly, we found that CD90^{hi} PDAC cells exhibited higher expression of PD-L1 compared with CD90^{-}

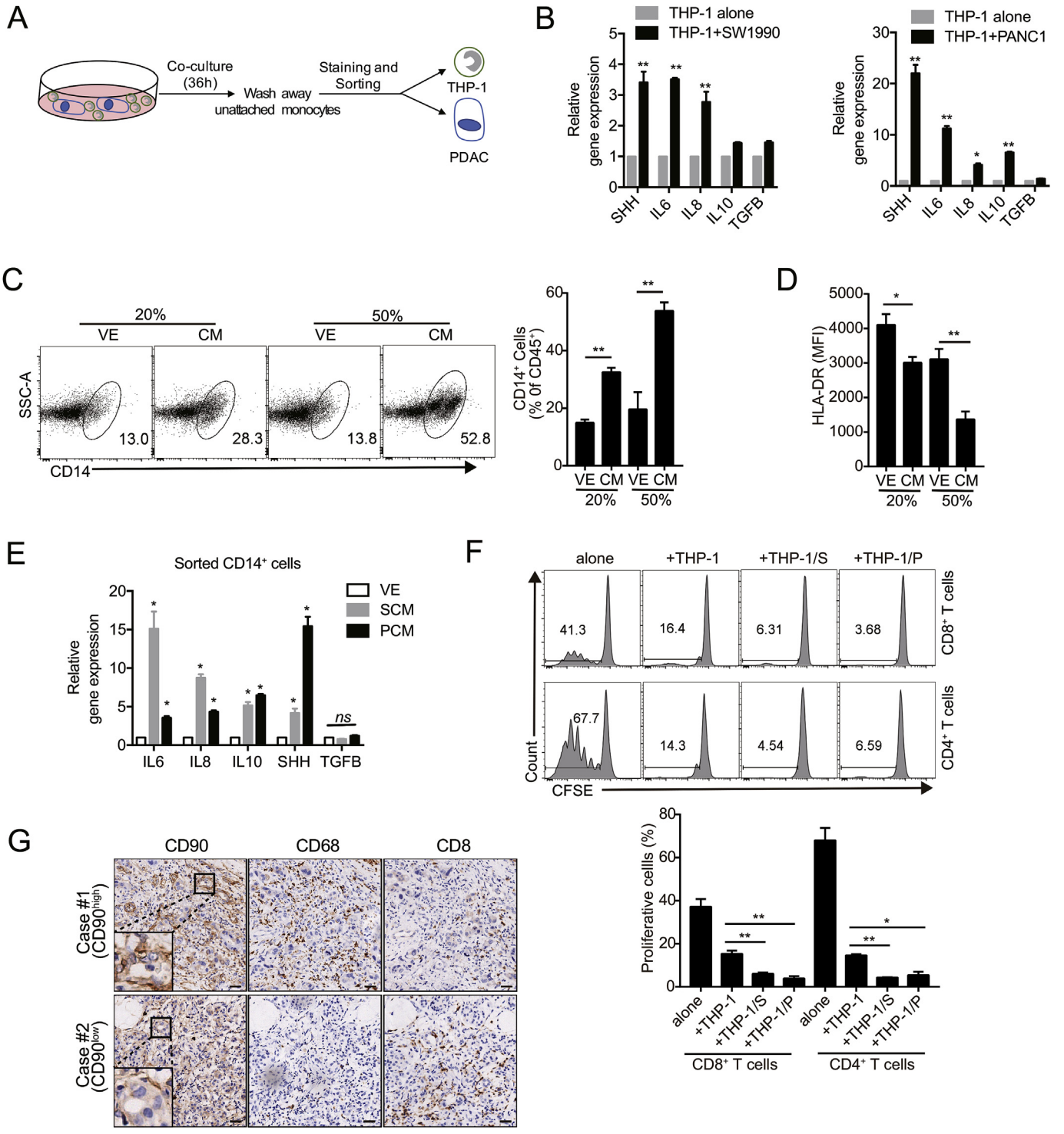

Fig. 4. PDAC cells promote immunosuppressive features of monocytes/macrophages. (A) Overview of the procedure to coculture PDAC cells with THP-1 monocytes. (B) THP-1 monocytes were cultured with or without PDAC cells for 36 h, and THP-1 monocytes were isolated for qPCR analysis. Bar graphs show the upregulation of SHH, IL6, and IL8 in THP-1 cells after coculture with PDAC cells. (C) PBMCs isolated from healthy donors were cocultured with PDAC conditioned medium in 96-well round bottom plates for 6 days. Representative flow cytometry plot shows that $CD14^+$ cells were upregulated after coculture with conditioned medium from PDAC cells. (D) Downregulation of HLA-DR expression upon PDAC_CM exposure. Flow cytometry was performed to examine HLA-DR expression on $CD14^+$ cells. (E) PBMCs from healthy donors were treated with PDAC conditioned medium in 6-well plates for 6 days. Then, $CD14^+$ cells were isolated by magnetic beads to examine the expression of the indicated genes by qPCR. (F) THP-1 monocytes were cultured with or without PDAC cells for 36 h. Then, THP-1 and primed THP-1 cells were isolated for coculture with CFSE-labeled $CD4^+$ and $CD8^+$ cells for 5 days. (G) Immunostaining of CD90, CD68 (macrophage marker) and CD8 ($CD8^+$ T cell marker) in PDAC tissues. All data are shown as the mean ± SD, Student's t-test, $^*P < 0.05$, $^{**}P < 0.01$, $^{***}P < 0.001$.

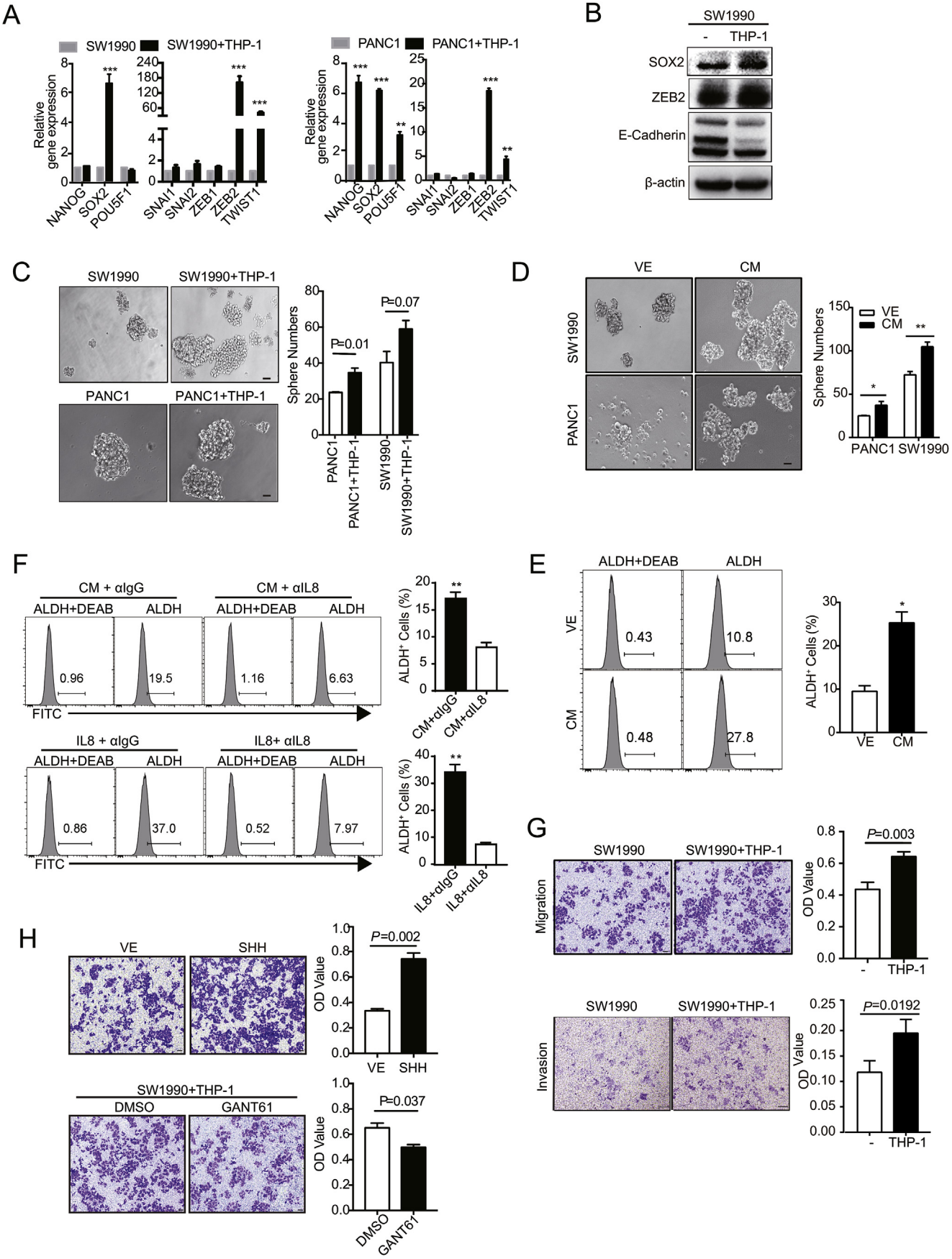

(caption on next page)

Fig. 5. Monocytes/Macrophages promote the stemness and EMT of PDAC cells (A, B) THP-1 monocytes were cultured with PDAC cells (SW1990 or PANC1) for 36 h. Then, PDAC cells were sorted for qPCR and western blot analyses. (C) A sphere assay was performed with sorted cells described in (A). Representative images and the number of spheres is shown (n ≥ 3, mean ± SEM). (D) A sphere assay was performed in SW1990 and PANC1 cells upon VE or THP-1 conditioned medium treatment. Representative images and the number of spheres is shown (n ≥ 3, mean ± SEM). (E) SW1990 cells were treated with VE or THP-1 CM for 36 h before ALDEFLUOR analyses. (F) ALDEFLUOR analyses of SW1990 cells after CM (top) or IL8 (bottom) treatment in the presence of αIgG or αIL8. Data represent the mean ± SEM. (G) THP-1 monocytes were cultured together with PDAC cells for 36 h. Then, cells were sorted for Transwell-based migration and invasion assays. (H) Migration rates of SW1990 cells upon SHH or VE treatment were evaluated with the migration assay. SW1990 cells were cocultured with THP-1 cells in the presence of GANT61 or DMSO treatment. SW1990 cells from 2 groups were sorted to perform the Transwell migration assay. Bar graphs depict the OD595 value of migrated cells (mean ± SEM of three independent experiments).

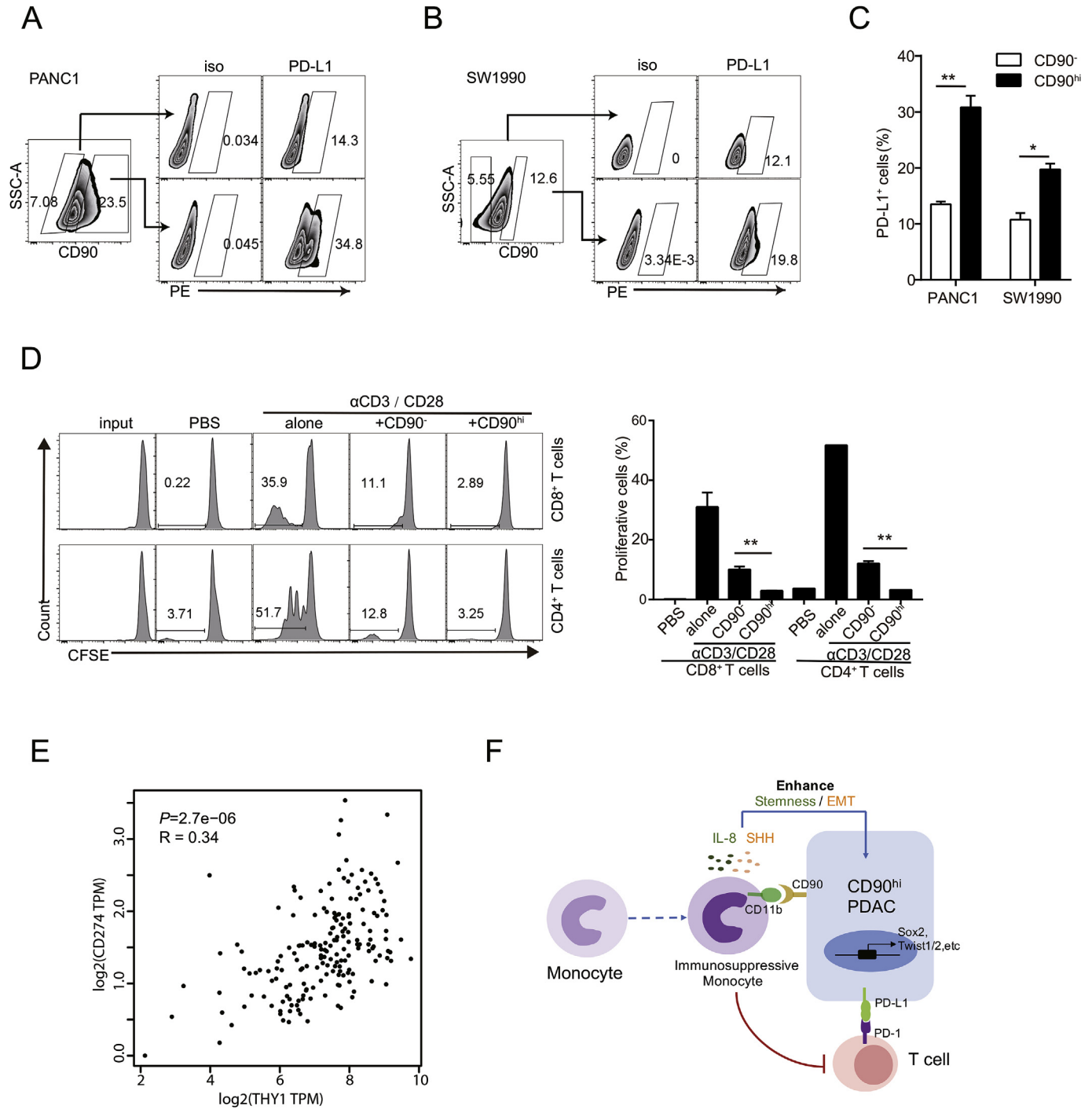

Fig. 6. CD90^{hi} PDAC cells exhibit high PD-L1 expression and suppress T cell proliferation (A, B) Representative flow cytometry plot showing the expression of PD-L1 in CD90^{hi} and CD90^{-} cells from PANC1 (A) and SW1990 (B) cells. (C) Bar graphs depict the high expression of PD-L1 in CD90^{hi} cells in both PANC1 and SW1990 cells. (D) CFSE-labeled CD4^{+} and CD8^{+} cells isolated from PBMCs were cocultured with CD90^{hi} or CD90^{-} cells for 5 days. A T cell suppression assay showed that CD90^{hi} cells could inhibit the proliferation of T cells. (E) Schematic graph depicting the crosstalk between CD90^{hi} PDAC cells and monocytes/macrophages and T cells.

cells (Fig. 6A–C), indicating a novel immune escape mechanism for the $CD90^{hi}$ population. To further verify our hypothesis, $CD4^+$ and $CD8^+$ T cells isolated from human PBMCs were cultured together with $CD90^{hi}$ and $CD90^-$ SW1990 cells, respectively. T cell proliferation was assessed by CFSE dilution. Compared with $CD90^-$ cells, $CD90^{hi}$ PDAC cells have a stronger inhibitory effect on T cell proliferation (both $CD4^+$ and $CD8^+$) (Fig. 6D). Moreover, a positive relationship between *THY1* (CD90) and *CD247* (PD-L1) mRNA levels was observed in TCGA (PAAD) database (Fig. 6E). Hence, the above results demonstrated the molecular mechanism by which CD90 mediated the crosstalk between pancreatic CSCs and surrounding monocytes/macrophages and T cells, which created an immunosuppressive microenvironment for PDAC progression (Fig. 6F).

4. Discussion

Cancer stem cells (CSCs) play an important role in the development and progression of pancreatic cancer. CSCs reside in niches, specialized microenvironments that protect them from the immune system and could enhance their stemness and metastatic potential [38,39]. The identification of pancreatic CSCs remains challenging. The investigation of CSCs and specialized microenvironments in which they thrive might provide novel therapeutic targets for pancreatic cancer. In our current study, we aimed to identify “stem-like” cells in pancreatic cancer and to investigate how these cells communicate with adjacent immune cells.

CD90 is a marker of mouse and human hematopoietic stem cells and has been described as a tumor-initiating cell marker in multiple solid tumors [16–20]. Previous reports have found that CD90 is expressed on stromal cells in PDAC tissues; however, its expression on PDAC cells has not yet been defined [21,22]. Here, using a pancreatic cancer tissue array from Renji Hospital, we confirmed that CD90 could be expressed on both stromal and tumor cells in PDAC. PDAC cell lines and primary cells were used to further confirm its expression on PDAC cells. To further understand how CD90 is involved in PDAC progression, GSEA was performed on the $CD90^{hi}$ and $CD90^{low}$ groups according to CD90 expression in PDAC patients. In line with the function of CD90 in other tumors, $CD90^{hi}$ PDAC samples showed a significant enrichment of genes upregulated in mammary stem cells. Moreover, by using a panel of stemness-related experiments, we further confirmed that the $CD90^{hi}$ population in PDAC harbored stemness properties with higher ALDH activity, sphere formation capability and tumorigenicity compared to $CD90^-$ cells. Given that CD90 is a plasma membrane receptor without an intracellular domain, it is unlikely to be a determinant for the stemness of PDAC cells. Instead, “stem-like cells” highly express CD90, which might be a strategy for them to enhance communication with surrounding cells.

The immunosuppressive microenvironment is a common feature in most solid tumors. Generally, the host immune system serves as a barrier against tumor formation. However, after transformation, immune cells are often redirected by tumor cells into an immunosuppressive state. This strategy is more necessary for CSCs to evade immune surveillance and sustain their stemness state. Recent years have seen immense progress in our understanding of how tumors interface with immune cells; however, few studies have shed light on how CSCs interact with immune cells in a manner different from non-CSCs. Tumor-associated macrophages (TAMs) and myeloid-derived suppressor cells (MDSCs) are responsible for immunosuppressive and tumor-promoting activity. CD90 is a GPI-anchored glycoprotein that interacts with integrins displayed by adjacent cells, such as the surface marker CD11b/MAC-1 (integrin alpha M/beta), which is expressed on monocytes/macrophages [31]. CD90, which is expressed on breast cancer stem cells, was shown to mediate the physical interaction between CSCs and macrophages and is one mechanism by which CSCs maintain their “stem-like” state. Here, in our current study, we found that $CD90^{hi}$ PDAC cells could tether and reprogram monocytes/macrophages into an immunosuppressive state; in turn, these monocytes/macrophages served to sustain the stemness/EMT features of PDAC cells. In addition to mediating physical interactions, very little is known about CD90 signaling capabilities. CD90 lacks an intracellular domain and hence is unable to transduce signals alone. Here, we found that CD90 acts as an anchor to enhance the communication between $CD90^{hi}$ PDAC cells and monocytes/macrophages in a near-secretory manner. However, other possibilities require further study, including whether CD90 could transactivate other receptors for signal transduction and whether the expression of CD90 on pancreatic stromal cells also mediates the crosstalk between monocytes/macrophages and stromal cells.

Programmed death-ligand 1 (PD-L1, also known as CD274 and B7-H1) is a critical “don't find me” signal to the adaptive immune system. Upregulation of PD-L1 is another strategy for tumor cells to evade the immune system. The suppression of PD-L1 to elicit an immune response against tumors has been translated to the clinic with very encouraging results. Here, our findings indicated that PD-L1 was dominantly expressed on $CD90^{hi}$ PDAC cells, a mechanism by which these “stem-like” cells avoid an adaptive immune response. As we have shown, CD90 could be regulated by Sonic Hedgehog and Hippo-YAP signaling. These two pathways have been reported to be associated with PD-L1 expression levels in tumors, which may explain the coexistence of PD-L1 and CD90 on PDAC cells.

Taken together, $CD90^{hi}$ “stem-like” cells created an immunosuppressive niche through reprogramming monocytes/macrophages and suppressing antitumor T cells directly, which favored the progression of pancreatic cancer. Elucidation of the crosstalk between immune cells and PDAC cells, especially pancreatic CSCs, would foster a better understanding of pancreatic cancer progression and provide a potential therapeutic strategy for targeting PDAC.

Conflicts of interest

All authors have declared that no conflict of interest exists.

Funding

This work was supported by Program for Professor of Special Appointment (Eastern Scholar) at Shanghai Institutions of Higher Learning No. TP2015007 (J. Xue), Shanghai Municipal Education Commission-Gaofeng Clinical Medicine Grant Support No. 20161312 (J. Xue), and the National Natural Science Foundation of China Nos. 81702938 and. 81770628 (J. Xue).

Acknowledgments

JJ.S. and J.X. designed the experiment, interpreted the data and wrote the manuscript; JJ.S. performed most of the experiments; P.L. and WY.S. assisted in some experiments; RZ.H. and MW.Y., under the supervision of YW.S., collected tissues from pancreatic cancer patients and organized their clinical information; T.F. assisted in some discussion; J.X., NN.N. and YW.S. provided an overall guide.

Appendix A. Supplementary data

Supplementary data to this article can be found online at https://doi.org/10.1016/j.canlet.2019.03.051.

References

[1] G. Bond-Smith, N. Banga, T.M. Hammond, C.J. Imber, Pancreatic adenocarcinoma, BMJ 344 (2012) e2476.
[2] Pancreatic Cancer Treatment (PDQ(R)): Health Professional Version, PDQ Cancer Information Summaries, Bethesda (MD), 2002.
[3] S. McGuire, World Cancer Report 2014, World Health Organization, International Agency for Research on Cancer, WHO Press, Geneva, Switzerland, 2015 Advances in nutrition, 7 (2016) 418-419.
[4] C. Li, D.G. Heidt, P. Dalerba, C.F. Burant, L. Zhang, V. Adsay, M. Wicha,

M.F. Clarke, D.M. Simeone, Identification of pancreatic cancer stem cells, Cancer Res. 67 (2007) 1030–1037.
[5] T. Reya, S.J. Morrison, M.F. Clarke, I.L. Weissman, Stem cells, cancer, and cancer stem cells, Nature 414 (2001) 105–111.
[6] R.N. Kaplan, R.D. Riba, S. Zacharoulis, A.H. Bramley, L. Vincent, C. Costa, D.D. MacDonald, D.K. Jin, K. Shido, S.A. Kerns, Z. Zhu, D. Hicklin, Y. Wu, J.L. Port, N. Altorki, E.R. Port, D. Ruggero, S.V. Shmelkov, K.K. Jensen, S. Rafii, D. Lyden, VEGFR1-positive haematopoietic bone marrow progenitors initiate the pre-metastatic niche, Nature 438 (2005) 820–827.
[7] R.T. Prehn, The immune reaction as a stimulator of tumor growth, Science 176 (1972) 170–171.
[8] H.A. Smith, Y. Kang, The metastasis-promoting roles of tumor-associated immune cells, J. Mol. Med. 91 (2013) 411–429.
[9] S. Takeuchi, M. Baghdadi, T. Tsuchikawa, H. Wada, T. Nakamura, H. Abe, S. Nakanishi, Y. Usui, K. Higuchi, M. Takahashi, K. Inoko, S. Sato, H. Takano, T. Shichinohe, K. Seino, S. Hirano, Chemotherapy-derived inflammatory responses accelerate the formation of immunosuppressive myeloid cells in the tissue microenvironment of human pancreatic cancer, Cancer Res. 75 (2015) 2629–2640.
[10] M.M. Kaneda, P. Cappello, A.V. Nguyen, N. Ralainirina, C.R. Hardamon, P. Foubert, M.C. Schmid, P. Sun, E. Mose, M. Bouvet, A.M. Lowy, M.A. Valasek, R. Sasik, F. Novelli, E. Hirsch, J.A. Varner, Macrophage PI3Kgamma drives pancreatic ductal adenocarcinoma progression, Cancer Discov. 6 (2016) 870–885.
[11] T. Cooks, I.S. Pateras, L.M. Jenkins, K.M. Patel, A.I. Robles, J. Morris, T. Forshew, E. Appella, V.G. Gorgoulis, C.C. Harris, Mutant p53 cancers reprogram macrophages to tumor supporting macrophages via exosomal miR-1246, Nat. Commun. 9 (2018) 771.
[12] Y. Zhu, J.M. Herndon, D.K. Sojka, K.W. Kim, B.L. Knolhoff, C. Zuo, D.R. Cullinan, J. Luo, A.R. Bearden, K.J. Lavine, W.M. Yokoyama, W.G. Hawkins, R.C. Fields, G.J. Randolph, D.G. DeNardo, Tissue-resident macrophages in pancreatic ductal adenocarcinoma originate from embryonic hematopoiesis and promote tumor progression, Immunity 47 (2017) 597.
[13] O. Helm, J. Held-Feindt, E. Grage-Griebenow, N. Reiling, H. Ungefroren, I. Vogel, U. Kruger, T. Becker, M. Ebsen, C. Rocken, D. Kabelitz, H. Schafer, S. Sebens, Tumor-associated macrophages exhibit pro- and anti-inflammatory properties by which they impact on pancreatic tumorigenesis, Int. J. Cancer 135 (2014) 843–861.
[14] A. Kumar, A. Bhanja, J. Bhattacharyya, B.G. Jaganathan, Multiple roles of CD90 in cancer, Tumour Biol.: the journal of the International Society for Oncodevelopmental Biology and Medicine 37 (2016) 11611–11622.
[15] T.A. Rege, J.S. Hagood, Thy-1 as a regulator of cell-cell and cell-matrix interactions in axon regeneration, apoptosis, adhesion, migration, cancer, and fibrosis, FASEB J. Off. Publ. Fed. Am. Soc. Exp. Biol. 20 (2006) 1045–1054.
[16] H. Lu, K.R. Clauser, W.L. Tam, J. Frose, X. Ye, E.N. Eaton, F. Reinhardt, V.S. Donnenberg, R. Bhargava, S.A. Carr, R.A. Weinberg, A breast cancer stem cell niche supported by juxtacrine signalling from monocytes and macrophages, Nat. Cell Biol. 16 (2014) 1105–1117.
[17] J. He, Y. Liu, T. Zhu, J. Zhu, F. Dimeco, A.L. Vescovi, J.A. Heth, K.M. Muraszko, X. Fan, D.M. Lubman, CD90 is identified as a candidate marker for cancer stem cells in primary high-grade gliomas using tissue microarrays, Mol. Cell. Proteomics: MCP 11 (2012) M111 010744.
[18] K.H. Tang, Y.D. Dai, M. Tong, Y.P. Chan, P.S. Kwan, L. Fu, Y.R. Qin, S.W. Tsao, H.L. Lung, M.L. Lung, D.K. Tong, S. Law, K.W. Chan, S. Ma, X.Y. Guan, A CD90(+) tumor-initiating cell population with an aggressive signature and metastatic capacity in esophageal cancer, Cancer Res. 73 (2013) 2322–2332.
[19] G.W. Krampitz, B.M. George, S.B. Willingham, J.P. Volkmer, K. Weiskopf, N. Jahchan, A.M. Newman, D. Sahoo, A.J. Zemek, R.L. Yanovsky, J.K. Nguyen, P.J. Schnorr, P.K. Mazur, J. Sage, T.A. Longacre, B.C. Visser, G.A. Poultsides, J.A. Norton, I.L. Weissman, Identification of tumorigenic cells and therapeutic targets in pancreatic neuroendocrine tumors, Proc. Natl. Acad. Sci. U. S. A. 113 (2016) 4464–4469.
[20] Z.F. Yang, D.W. Ho, M.N. Ng, C.K. Lau, W.C. Yu, P. Ngai, P.W. Chu, C.T. Lam, R.T. Poon, S.T. Fan, Significance of CD90+ cancer stem cells in human liver cancer, Cancer Cell 13 (2008) 153–166.
[21] X. Pei, J. Zhu, R. Yang, Z. Tan, M. An, J. Shi, D.M. Lubman, CD90 and CD24 Co-expression is associated with pancreatic intraepithelial neoplasias, PLoS One 11 (2016) e0158021.
[22] J. Zhu, S. Thakolwiboon, X. Liu, M. Zhang, D.M. Lubman, Overexpression of CD90 (Thy-1) in pancreatic adenocarcinoma present in the tumor microenvironment, PLoS One 9 (2014) e115507.
[23] X. Wang, X. Lu, T. Zhang, C. Wen, M. Shi, X. Tang, H. Chen, C. Peng, H. Li, Y. Fang, X. Deng, B. Shen, mir-329 restricts tumor growth by targeting grb2 in pancreatic cancer, Oncotarget 7 (2016) 21441–21453.
[24] P.C. Hermann, S.L. Huber, T. Herrler, A. Aicher, J.W. Ellwart, M. Guba, C.J. Bruns, C. Heeschen, Distinct populations of cancer stem cells determine tumor growth and metastatic activity in human pancreatic cancer, Cell stem cell 1 (2007) 313–323.
[25] E. Lonardo, P.C. Hermann, M.T. Mueller, S. Huber, A. Balic, I. Miranda-Lorenzo, S. Zagorac, S. Alcala, I. Rodriguez-Arabaolaza, J.C. Ramirez, R. Torres-Ruiz, E. Garcia, M. Hidalgo, D.A. Cebrian, R. Heuchel, M. Lohr, F. Berger, P. Bartenstein, A. Aicher, C. Heeschen, Nodal/Activin signaling drives self-renewal and tumorigenicity of pancreatic cancer stem cells and provides a target for combined drug therapy, Cell stem cell 9 (2011) 433–446.
[26] J. Zhou, M. Liu, H. Sun, Y. Feng, L. Xu, A.W.H. Chan, J.H. Tong, J. Wong, C.C.N. Chong, P.B.S. Lai, H.K. Wang, S.W. Tsang, T. Goodwin, R. Liu, L. Huang, Z. Chen, J.J. Sung, K.L. Chow, K.F. To, A.S. Cheng, Hepatoma-intrinsic CCRK inhibition diminishes myeloid-derived suppressor cell immunosuppression and enhances immune-checkpoint blockade efficacy, Gut 67 (2018) 931–944.
[27] L. Badea, V. Herlea, S.O. Dima, T. Dumitrascu, I. Popescu, Combined gene expression analysis of whole-tissue and microdissected pancreatic ductal adenocarcinoma identifies genes specifically overexpressed in tumor epithelia, Hepato-Gastroenterology 55 (2008) 2016–2027.
[28] L. Vrba, J.C. Garbe, M.R. Stampfer, B.W. Futscher, Epigenetic regulation of normal human mammary cell type-specific miRNAs, Genome Res. 21 (2011) 2026–2037.
[29] W. He, J. Wu, J. Shi, Y.M. Huo, W. Dai, J. Geng, P. Lu, M.W. Yang, Y. Fang, W. Wang, Z.G. Zhang, A. Habtezion, Y.W. Sun, J. Xue, IL22RA1/STAT3 signaling promotes stemness and tumorigenicity in pancreatic cancer, Cancer Res. 78 (2018) 3293–3305.
[30] T. Crnogorac-Jurcevic, C. Chelala, S. Barry, T. Harada, V. Bhakta, S. Lattimore, S. Jurcevic, M. Bronner, N.R. Lemoine, T.A. Brentnall, Molecular analysis of precursor lesions in familial pancreatic cancer, PLoS One 8 (2013) e54830.
[31] A. Wetzel, T. Chavakis, K.T. Preissner, M. Sticherling, U.F. Haustein, U. Anderegg, A. Saalbach, Human Thy-1 (CD90) on activated endothelial cells is a counterreceptor for the leukocyte integrin Mac-1 (CD11b/CD18), J. Immunol. 172 (2004) 3850–3859.
[32] L. Chen, J. Fan, H. Chen, Z. Meng, Z. Chen, P. Wang, L. Liu, The IL-8/CXCR1 axis is associated with cancer stem cell-like properties and correlates with clinical prognosis in human pancreatic cancer cases, Sci. Rep. 4 (2014) 5911.
[33] C. Huang, Z. Li, N. Li, Y. Li, A. Chang, T. Zhao, X. Wang, H. Wang, S. Gao, S. Yang, J. Hao, H. Ren, Interleukin 35 expression correlates with microvessel density in pancreatic ductal adenocarcinoma, recruits monocytes, and promotes growth and angiogenesis of xenograft tumors in mice, Gastroenterology 154 (2018) 675–688.
[34] F. Liotti, F. Collina, E. Pone, L. La Sala, R. Franco, N. Prevete, R.M. Melillo, Interleukin-8, but not the related chemokine CXCL1, sustains an autocrine circuit necessary for the properties and functions of thyroid cancer stem cells, Stem Cell. 35 (2017) 135–146.
[35] G. Feldmann, S. Dhara, V. Fendrich, D. Bedja, R. Beaty, M. Mullendore, C. Karikari, H. Alvarez, C. Iacobuzio-Donahue, A. Jimeno, K.L. Gabrielson, W. Matsui, A. Maitra, Blockade of hedgehog signaling inhibits pancreatic cancer invasion and metastases: a new paradigm for combination therapy in solid cancers, Cancer Res. 67 (2007) 2187–2196.
[36] K. Zhang, S. Che, C. Pan, Z. Su, S. Zheng, S. Yang, H. Zhang, W. Li, W. Wang, J. Liu, The SHH/Gli axis regulates CD90-mediated liver cancer stem cell function by activating the IL6/JAK2 pathway, J. Cell Mol. Med. 22 (2018) 3679–3690.
[37] A. Wu, J. Wei, L.Y. Kong, Y. Wang, W. Priebe, W. Qiao, R. Sawaya, A.B. Heimberger, Glioma cancer stem cells induce immunosuppressive macrophages/microglia, Neuro Oncol. 12 (2010) 1113–1125.
[38] D.O. Croci, M.F. Zacarias Fluck, M.J. Rico, P. Matar, G.A. Rabinovich, O.G. Scharovsky, Dynamic cross-talk between tumor and immune cells in orchestrating the immunosuppressive network at the tumor microenvironment, Canc. Immunol. Immunother: CII 56 (2007) 1687–1700.
[39] F. Spill, D.S. Reynolds, R.D. Kamm, M.H. Zaman, Impact of the physical microenvironment on tumor progression and metastasis, Curr. Opin. Biotechnol. 40 (2016) 41–48.